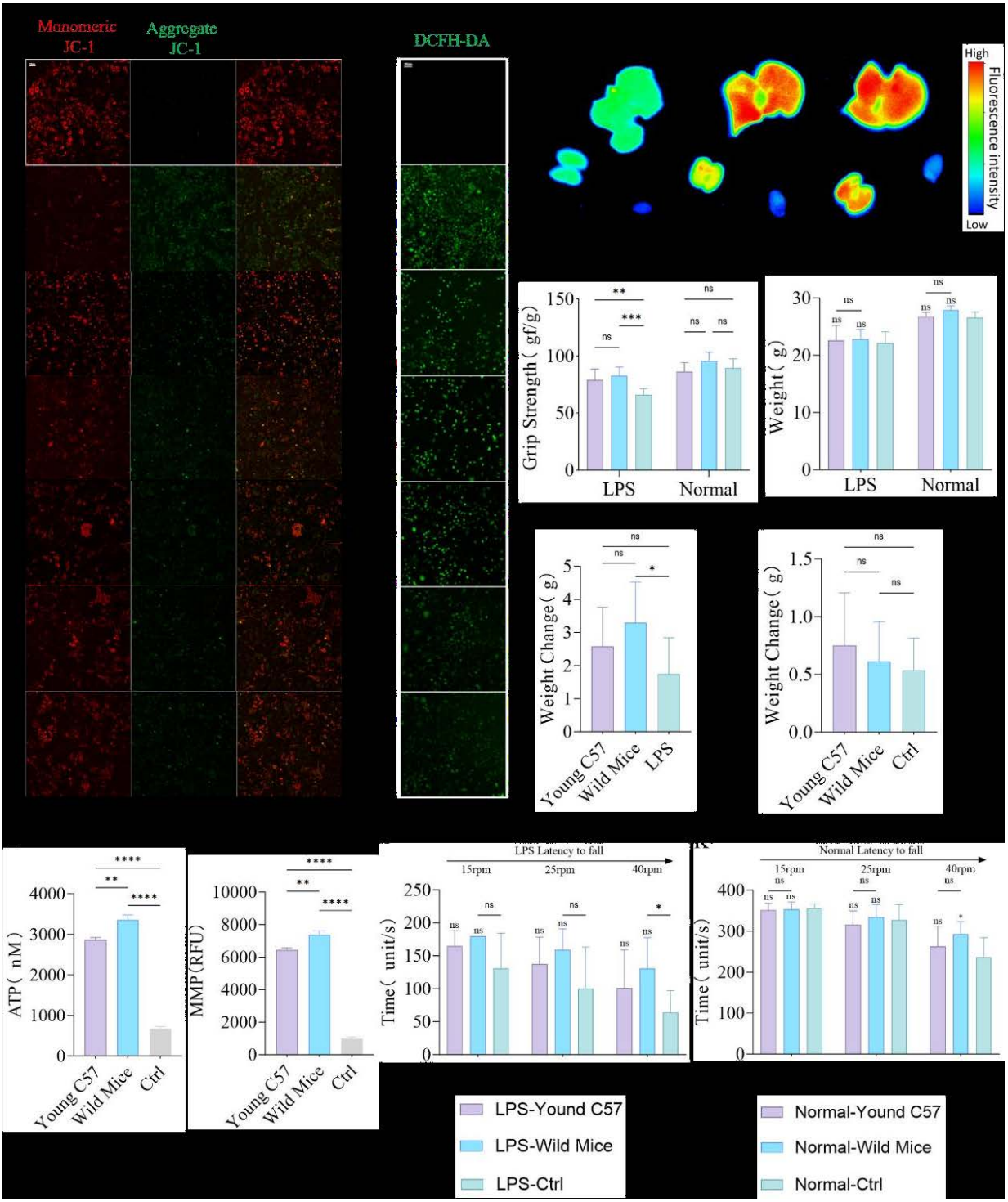

Figure 6: Mitochondrial transplantation enhances physical function.

■ Outcomes

- A: Fluorescence imaging of mitochondrial membrane potential in HepG2 cells treated with CCCP 24 hours after transplantation of five different mitochondria, with untreated cells as control. Scale bar: 30 μm.
- B: Fluorescence imaging of Reactive Oxygen Species (ROS) in HepG2 cells treated with CCCP after transplantation of five different mitochondria, with untreated cells as control. Scale bar: 30 μm.
- C-D: Evaluation of isolated mitochondria functions via ATP production and Mitochondrial Membrane Potential (MMP) assays, with mitochondria

subjected to two freeze-thaw cycles at -80°C and 37°C to completely disrupt structure and function as control.

- E: Biodistribution of exogenous mitochondria in mouse liver, kidney, and heart detected by in vivo imaging. 24 hours after intravenous tail vein injection of mitochondria. Blank: untreated LPS model group mice.
- F-H: Body weight changes in acute inflammation model mice and normal mice before and one week after transplantation of two different mitochondria, with untreated groups as control.Grip strength measurement in acute inflammation model mice and normal mice three days after transplantation of two different mitochondria, with untreated groups as control.
- J-K: Motor function assessment in acute inflammation model mice and normal mice three days after transplantation of two different mitochondria, with untreated groups as control.

ns = no statistical significance, * = p<0.05, ** = p<0.01, *** = p<0.001, **** = p<0.0001

Co-culturing mitochondria from each group with normal BMDM enhanced their bioenergetic capacity, with the Wild Mice group showing the most significant ATP increase (Figure 5C). Both mitochondrial types improved cell viability in LPS-treated BMDM and reduced mitochondrial ROS production, with the Wild Mice group demonstrating better oxidative stress relief and cell viability enhancement (Figures 7L-7N). The second animal experiment provided a more comprehensive validation. While the Young C57 group showed good results, the Wild Mice group exhibited superior therapeutic effects in the acute inflammation model and LPS-treated BMDM, further enhancing cellular bioenergetics and demonstrating the potential of mitochondrial transplantation in boosting biological function.

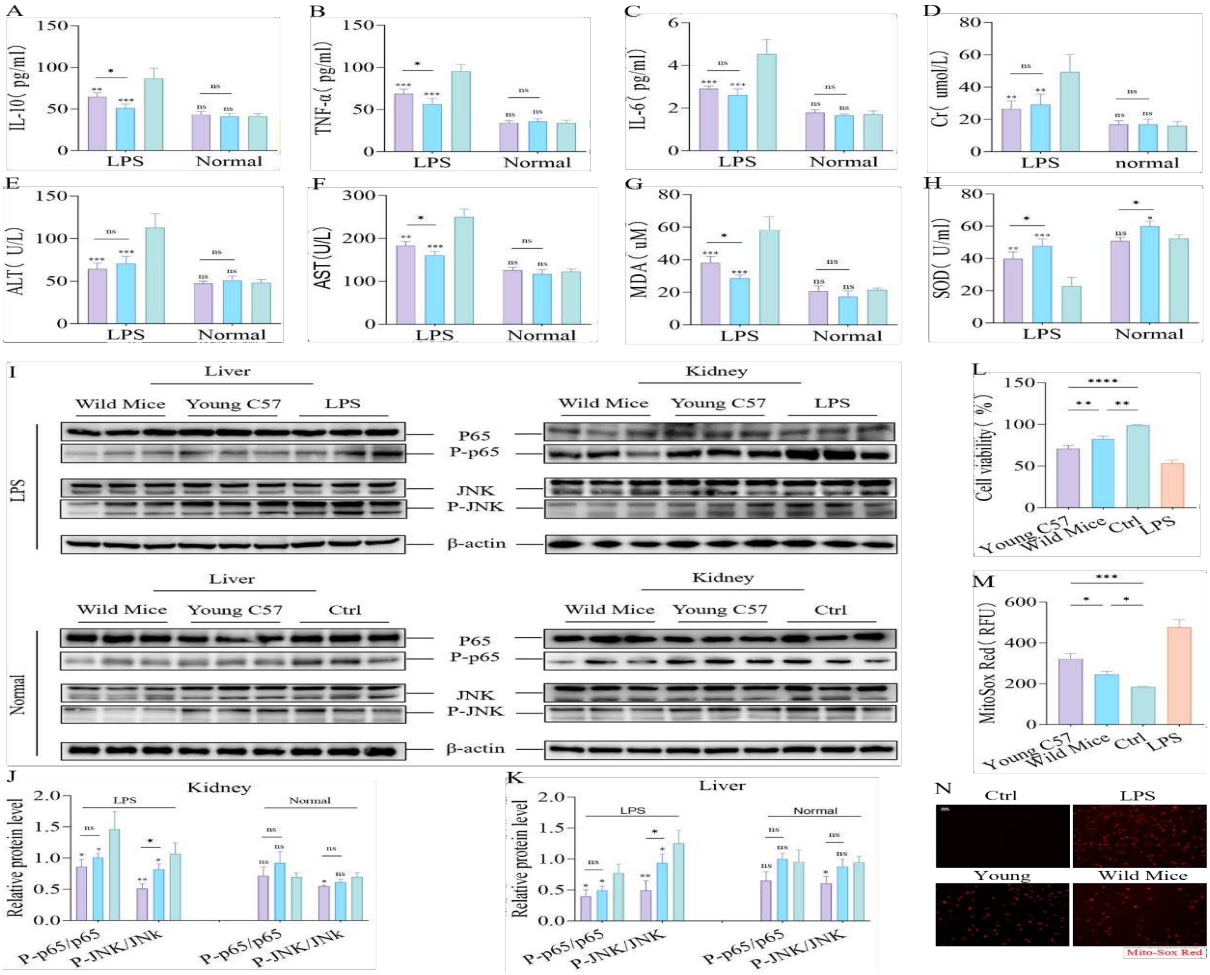

Figure 7: Mitochondrial transplantation enhances biological potency in mice.

Outcomes

- A-C Changes in serum levels of IL-6, TNF-α, and IL-10 in acute inflammation model mice and normal mice one week after transplantation of two different mitochondria, with untreated groups as control.
- D-F Evaluation of kidney and liver function via serum Cr, ALT, and AST levels in acute inflammation model mice and normal mice one week after transplantation of two different mitochondria, with untreated groups as control.
- G-H: Measurement of serum MDA levels and SOD activity in acute inflammation model mice and normal mice one week after transplantation of two different mitochondria, with untreated groups as control.
- I-K: Analysis of JNK and P-JNK, p65, and P-p65 protein expression levels in liver and kidney tissues via Western blot one week after transplantation of two different mitochondria in acute inflammation model mice and normal mice, with untreated groups as control.
- L Effects of two different mitochondria on the viability of LPS-treated BMDM cells 24 hours after transplantation, with untreated groups as control.
- M-N Fluorescence imaging and quantitative analysis of mitochondrial ROS levels in LPS-treated BMDM cells 24 hours after transplantation of two different mitochondria, with untreated groups as control. Scale bar: 30 μm.

ns = no statistical significance, * = $p<0.05$, ** = $p<0.01$, *** = $p<0.001$, **** = $p<0.0001$

Results and Discussion

The endosymbiotic nature of mitochondria grants them a unique non-immunogenic profile. The adaptation of organisms to their environments has resulted in mitochondria with unique functions, such as cytoplasmic male sterility in plants and drug resistance in eukaryotic cells, both of which are associated with mt DNA. Some mitochondrial functions remain unexplained, yet this does not hinder our exploration of mitochondrial transplantation [62-64]. Transplanted mitochondria need to be metabolically compatible with recipient cells. If recipient cells acquire exogenous mitochondria with lineage-specific characteristics that match their metabolism and can adapt to different stimuli, could we harness different functions from mitochondria of various lineages? Could we, by extension, fuse and absorb unique functions from diverse organisms to accelerate evolution? Given that cells develop tolerance to various stimuli and drugs, could mitochondrial transplantation also develop tolerance? Repeated transplantation of the same type of mitochondria may gradually diminish its effects. Could we, therefore, obtain more potent mitochondria to avoid tolerance and allow the recipient to gradually adapt and enhance biological functions?

Therefore, I designed a series of experiments. The successful internalization of 14 different biological mitochondria by 3 types of cells, compared to previous studies, further confirms the universality and safety of mitochondrial transplantation, while expanding the sources of mitochondria. I hope this can provide patients with more diverse options. I further used 3 cell types and 4 disease models in various combinations to explore the possibility of merging mitochondrial characteristics from different sources. It appears that the source of mitochondria is not significantly restricted, allowing us to screen for mitochondria from different species that are more metabolically compatible and suitable for disease treatment. Since we can assimilate the characteristics of one type of mitochondria, we might also be able to assimilate the characteristics of multiple types. The hybrid mitochondria from HL1 and H9C2 lines exhibited stronger therapeutic effects compared to either HL1 or H9C2 alone, suggesting that it might be possible to artificially create such hybrid mitochondria to target specific diseases. For example, mitochondria from scavengers like Komodo dragons and vultures might have enhanced antibacterial capabilities, while those from honey badgers or mongoose could possess better anti-venom properties. We could potentially combine these characteristics for targeted therapies, or even create multi- species hybrid mitochondria similar to multi-drug-resistant bacteria as a universal therapeutic approach. However, these approaches are based on the premise that the functional differences between the mitochondria used are not significant. For the average patient, single-lineage mitochondrial matching might be more appropriate due to safety concerns. As we aim to explore the potential of mitochondrial transplantation and find better therapeutic methods, I have further demonstrated the significant advantages of powerful mitochondria over metabolic matching in

mitochondrial transplantation. These results suggest that the primary therapeutic effect of mitochondrial transplantation may be more related to the rescue of bioenergetics, with changes in cellular metabolism and proteomics being secondary.

We did not perform mitochondrial transplantation on the same batch of cells under different stimuli because the biological function of mitochondria is more critical than metabolic matching. Future research should focus on identifying more potent mitochondria for therapeutic applications. Although metabolic matching is currently important, especially from a safety perspective, it can serve as a foundation for mitochondrial fusion experiments to explore diverse biological therapies. In an artificially cultured environment, especially in stem cells where mitochondrial DNA oxidative damage accumulates less, the significant functional advantages of potent mitochondria may outweigh this benefit. While stem cells are a suitable source due to safety considerations, I believe that future mitochondrial transplantation would be more effective when based on a background of multiple germline sources, optimizing treatment options for metabolic matching. I cannot guarantee the absolute correctness of the current experiments, as the cumulative quantitative changes from multi-lineage hybrid mitochondrial transplantation might surpass the benefits brought by mitochondrial quality itself. Even now, I wouldn't claim that my research is entirely accurate; my experiments emphasize the possibilities of the future, particularly the potential for bio-enhancement.

The results of animal experiments were largely consistent with those of cell experiments, where mitochondria with various functional strengths demonstrated significant therapeutic effects. Notably, Wild Mice mitochondria were more effective in disease model mice and cells compared to other mitochondria. Although the Trained C57 mitochondria did not exhibit the same pronounced therapeutic effects as Wild Mice, their overall therapeutic enhancement was superior to other groups. The Trained People mitochondria did not show the expected therapeutic outcomes, which I attribute to my own suboptimal health due to prolonged lab work, leading to a slightly weaker enhancement of mitochondrial function compared to Trained C57. However, neither Young C57 nor Trained People mitochondria showed a significant difference in therapeutic effect compared to C2C12, suggesting that in vivo mitochondria might compensate for the lower therapeutic efficacy associated with lower DNA oxidative damage in cellular mitochondria. We also observed an enhancement in the biological functions of normal cells by Wild Mice mitochondria, even improving the physiological functions of normal mice to some extent. Additionally, in these two mitochondrial transplantation pre-treatment cell experiments, we observed an increase in recipient cell ATP energy as mitochondrial function improved. This suggests a new solution to mitochondrial transplantation tolerance and potentially an optimized approach for multiple mitochondrial transplants. Importantly, our current results do not indicate a limit to the therapeutic effects of mitochondrial transplantation, implying that we can continue to explore more powerful mitochondria to better assist in treatment, and potentially even enhance human biological functions to some extent. This represents a significant expansion of the implications of mitochondrial transplantation, and I believe that my research could provide stronger and more diverse therapeutic options for clinical applications.

Methods

Cell lines

Bovine kidney cells, porcine kidney cells, African green monkey kidney cells, feline kidney cells, canine kidney cells, human cardiomyocytes, rat cardiomyocytes, mouse cardiomyocytes, and human hepatocellular carcinoma cells were obtained from the Cell Center of the Chinese Academy of Sciences (China). Chicken hepatocellular carcinoma cells were purchased from Sunncell (China), and Spodoptera frugiperda cells and mouse fibroblasts were purchased from Procell (China). The bovine kidney cells, porcine kidney cells, African green monkey kidney cells, feline kidney cells, canine kidney cells, chicken hepatocellular carcinoma cells, human cardiomyocytes, rat cardiomyocytes, mouse cardiomyocytes, mouse myoblasts, and human hepatocellular carcinoma cells were cultured in Dulbecco's Modified Eagle Medium (DMEM) (Gibco) supplemented with 10% (v/v) fetal bovine serum (Gibco) and 1% (v/v) penicillin-streptomycin (Gibco) and incubated at 37°C in a humidified atmosphere with 5% CO_2. Spodoptera frugiperda cells were cultured in SF-900TM II SEM (Gibco) medium in a shaker flask at 28°C.

Animals

The animal experiments involved in this study were all C57 B/L 6J strains purchased from the Animal Protection Center of Southern Medical University. All mice were maintained in a specific pathogen-free SPF environment. All mice were used in accordance with the scheme approved by the Review

Committee of Southern Medical University. The mouse experimental scheme has been approved by the Animal Care and Use Committee of Southern Medical University, and the experimental animal facilities have been licensed by the Guangdong Medical Experimental Animal Center (SCXK-2021-0041). Lizards, salmon, bullfrogs, parakeets, turtles, and eels were purchased from animal breeding markets. Wild mice were captured using traps in the wild, disinfected, and then housed in the laboratory under appropriate conditions.

■ Human subjects

The human subject involved in this study was the author. Full informed consent was obtained, and muscle tissue was surgically collected from the gastrocnemius muscle following ethical guidelines approved by the Ethics Review Board of Southern Medical University.

■ Plants

Vaucheria litorea was collected and transported under expert supervision and used immediately after thorough disinfection.

■ Isolation of mouse Bone Marrow-Derived Macrophages (BMDMs)

Bones were aseptically harvested from the hind legs of C57BL/6 mice, and muscle tissues were removed. Bone marrow was flushed out of the bones using a 25-gauge needle attached to a syringe containing BMDM growth medium, which consists of DMEM, 20% L929 cell- conditioned medium to generate M-CSF, 10% FBS, and 1% penicillin/streptomycin. BMDMs were allowed to differentiate for 7 days at 37°C with 5% CO_2, with the growth medium changed every 2 days during ex vivo culture.

■ Establishment of cell disease models

Oxidative stress models were established by treating AC16 with 500 μM H_2O_2 for 24 hours and HepG2 cells with 700 μM H_2O_2 for 24 hours. Inflammation models were established by treating BMDM cells with 100nM LPS for 24 hours and HepG2 cells with 1 μM LPS for 24 hours. Mitophagy models were established by treating AC16 and HepG2 cells with 30 μM CCCP for 24 hours. Senescence model was established by treating HepG2 cells with 30 g/L D-gal for 48 hours.

■ Disinfection and sterilization of plant mitochondria

Weigh 1g of tissue and rinse with clean water for 3 hours. Transfer to a laminar flow hood, soak in 75% ethanol for 1 minute, then wash twice with DPBS containing 1% streptomycin/penicillin. After soaking in 2% sodium hypochlorite (NaClO) for 8 minutes, wash three times with DPBS containing 1% streptomycin/penicillin for 1 minute each time. Then, rinse repeatedly in 1% $MgCl_2$ solution for 10 minutes. After that, wash three times with DPBS containing 1% streptomycin/penicillin. Place the sterilized tissue blocks into a 100 mm^2 culture dish (Corning) and cut them into 0.1 cm^2 pieces for further use.

■ Mitochondrial isolation

Mitochondria were isolated from cultured cells, animal tissues, and plant tissues using the Mitochondria-Cytosol Protein Isolation Kit (C0010-50, Applygen) and the Plant Mitochondrial Extraction Kit (SM0020, Solarbio). For tissue homogenization, 100 mg–200 mg of fresh animal tissue or 1 g of plant tissue was cut into 0.5 cm^2 pieces and placed into a Teflon-glass homogenizer with 2.5 ml of ice-cold mitochondrial extraction buffer. The tissue was homogenized 20 times using a tight-fitting pestle. For cell homogenization, 2.5× 10^7 cells were collected, digested, centrifuged, washed, and resuspended in 1.5 ml of ice- cold mitochondrial extraction buffer. The cell suspension was transferred to a small glass homogenizer and homogenized 30 times using a tight-fitting pestle. The homogenate was transferred to a centrifuge tube and centrifuged at 800 × g for 5 minutes at 4°C. The supernatant was collected and transferred to a new centrifuge tube and centrifuged at 10,000 × g for 10 minutes at 4°C. The mitochondrial pellet was resuspended in 0.2 ml of mitochondrial extraction buffer, followed by centrifugation at 12,000 × g for 10 minutes at 4°C. The supernatant was discarded, and the mitochondrial pellet was resuspended in mitochondrial respiration buffer for subsequent use.

■ Mitochondrial quality control

The extracted mitochondria were quantified using a BCA Protein Assay Kit (23250, ThermoFisher). The integrity of the isolated mitochondria was assessed using the Mitochondrial Complex I(E-BC-K151-M , Elabscience) and III Activity Assay Kit (E-BC- K149-M , Elabscience), the mitochondrial membrane potential was measured using the Mitochondrial Membrane Potential Assay Kit with JC-1 (C2006, Byeotime), and the energy synthesis capacity was evaluated using an ATP Assay Kit (S0026, Byeotime).

■ Electron microscopy

For Transmission Electron Microscopy (TEM), the isolated mitochondria were fixed overnight in 0.2 M sodium cacodylate buffer containing 2.5% formaldehyde, 5% glutaraldehyde, and 0.06% picric

acid at pH 7.4. The samples were washed in cacodylate buffer, stained with 1% osmium tetroxide and 1.5% potassium ferricyanide, and then dehydrated using ethanol and propylene oxide. After infiltration and embedding in Epon- Araldite (Electron Microscopy Sciences, Hatfield, PA), sections (60 nm-80 nm thick) were cut using an Ultracut-S ultramicrotome (Reichert Technologies, Depew, NY) and mounted on copper grids (200 mesh) for observation with a transmission electron microscope (Hitachi H-7500).

■ Mitochondrial transplantation in cells

After mitochondrial isolation, the mitochondria were quantified using a BCA Protein Assay Kit (23250, ThermoFisher). For co-culture, 10 μg of mitochondria were added per 107 cells. For competitive mitochondrial internalization, 1 μg of mitochondria was added per 107 cells, with 0.5 μg of each type for dual mitochondrial competition or 0.33 μg of each type for triple mitochondrial competition.

■ Mitochondrial internalization and observation

Recipient cell membranes were labeled with WGA594 or WGA488, and the isolated exogenous mitochondria were labeled with MitoTracker™ Green FM or MitoTracker™ Red CMXRos. Both the cells and the exogenous mitochondria were washed twice with DPBS after 30 minutes. The mitochondria and cells were co-cultured for 24 hours in confocal dishes, fixed with paraformaldehyde containing DAPI, washed twice with DPBS, and observed using an inverted laser confocal microscope (LSM900 with Airyscan2, Zeiss).

■ ATP content measurement

ATP content was measured using an ATP Assay Kit (S0026, Beyotime) following the manufacturer's instructions. One hundred micrograms of isolated mitochondria or cells seeded in a 6-well plate (at a density of 5×10^7 cells/well) were treated with 200 μL of ATP lysis buffer, centrifuged at 12,000 × g for 5 minutes at 4°C. Twenty microliters of supernatant were mixed with 100 μL of ATP detection solution in a 96-well white solid flat-bottom polystyrene microplate (Corning) and the luminescence (RLU) was measured using a multifunctional microplate reader (Tecan).

■ Mitochondrial membrane potential fluorescence quantification

The isolated mitochondria were subjected to protein quantification, followed by mitochondrial membrane potential assessment using the Mitochondrial Membrane Potential Assay Kit with JC-1 (C2006, Byeotime). In brief, 50 μg of mitochondria were mixed with 90 μL of JC-1 staining solution (2 μM) and seeded into a 96-well plate. The mixture was thoroughly mixed, and the membrane potential was immediately measured using the BioTek Cytation5 Multifunctional Cell Imaging Microplate Reader (Agilent), with an excitation wavelength of 485 nm and an emission wavelength of 590 nm.

■ Measurement of intracellular reactive oxygen species

Cells were seeded at a density of 1×10^7 cells/well in a 24-well plate. After treating the cells with the respective conditions, exogenous mitochondria were co-cultured with the cells for 24 hours. The medium was then removed, and the cells were washed twice with DPBS. The cells were incubated with 10 μM DCFH-DA (Beyotime) or 5 μM MitoSOX Red at 37°C for 30 minutes. The stained cells were washed with PBS and observed using an inverted laser scanning confocal microscope (LSM900 with Airyscan2, Zeiss) or an inverted fluorescence microscope (EVOS M5000, ThermoFisher). The mitochondrial ROS fluorescence intensity was measured using a multifunctional microplate reader (Tecan) with an excitation wavelength of 510 nm and an emission wavelength of 580 nm.

■ Measurement of mitochondrial membrane potential

Cells were seeded at a density of 1×10^7 cells/well in a 24-well plate. After treating the cells with the respective conditions, exogenous mitochondria were co-cultured with the cells for 24 hours. The medium was then removed, and the cells were washed twice with DPBS. Following the Mitochondrial Membrane Potential Assay Kit with JC-1 protocol, 500 μL of JC-1 staining solution (2 μM) was added to each well and incubated for 20 minutes. The cells were then washed and observed using an inverted laser scanning confocal microscope (LSM900 with Airyscan2, Zeiss) or an inverted fluorescence microscope (EVOS M5000, ThermoFisher) in phenol-red-free DMEM (Invitrogen).

■ CCK8 assay

According to the Cell Counting Kit-8 (C0037, Beyotime) protocol, 100 μL of cell suspension (density of 1×10^4) was seeded in a 96-well plate. After treating the cells with the respective conditions, 10 μL of CCK8 reagent was added, and the cells were incubated at 37°C for 2 hours. The absorbance at 450 nm was measured using a multifunctional microplate reader (Tecan). The percentage of cell viability was calculated based on the average Optical Density (OD) of each group.

■ DNA oxidative damage detection

The supernatant of the cultured cells was collected 24 hours after mitochondrial transplantation. The 8-OHdG concentration was measured using the 8-OHdG ELISA Kit (E-EL-0028, Elabscience), and absorbance at 450 nm was recorded to quantify DNA oxidative damage.

■ Immunoinflammatory cytokines detection

The supernatant of the cultured cells was collected 24 hours after mitochondrial transplantation. The concentrations of IL-6, IL-10, and TNF-α were measured using the Mouse IL-6 ELISA Kit (PI326, Byeotime), Mouse IL-10 ELISA Kit (PI522, Byeotime), and Mouse TNF-α ELISA Kit (PT512, Byeotime), respectively, according to the manufacturer's instructions, with absorbance at 450 nm.

■ Measurement of NOS, MDA, GSH, SOD, ALT, AST, Cr

The supernatants of cultured cells post-mitochondrial transplantation or serum from model mice were collected. According to the manufacturer's instructions (NJJCBIO), the OD values for NOS(A014-2-2), MDA(A003-1-2), GSH(A005-1-2), SOD(A001-2-2), ALT(C010-2-1), AST(C009-2-1), and Cr(C011-2-1) were measured at 550 nm, 532 nm, 412 nm, 550 nm, 505 nm, 510 nm, and 546 nm, respectively.

■ Cell fusion

When cells reached high proliferation rates and good condition, 3×10^6 HL-1 and H9C2 cells were harvested separately. HL1 cells were stained with WGA647 and H9C2 cells with WGA594. The staining was performed at 37°C for 25 minutes, followed by two washes with DPBS. The cells were then mixed and centrifuged at 200 g for 5 minutes. The supernatant was removed, and pre-warmed 50% PEG1450 (P7181, Sigma) was gradually added while stirring the pellet. A total of 700 μL of 50% PEG1450 was added within 1 minute. The mixture was incubated at 37°C for 1 minute, and then 10 mL of DMEM was added to dilute the PEG1450. The centrifuge tube was placed in a 37°C incubator for 10 minutes before being centrifuged again at 200 g for 5 minutes. The cells were washed twice with DPBS, resuspended in complete culture medium, and incubated at 37°C with 5% CO_2 for 24-48 hours. Cell fusion was observed using an inverted laser scanning confocal microscope (LSM900 with Airyscan2, Zeiss), and fused HL1+H9C2 cells were sorted using a MoFlow XDP flow sorter (Beckman) for further culture.

■ Mitochondrial competitive internalization

For two types of mitochondrial competitive internalization, the mitochondria were stained with MitoTracker™ Deep Red FM and MitoTracker™ Green FM for 30 minutes, washed twice with DPBS, and co-cultured with recipient cells for 24 hours. The medium was replaced with phenol-red-free culture medium containing ProlongTM antifade reagent, and live-cell imaging was performed using an inverted laser scanning confocal microscope (LSM900 with Airyscan2, Zeiss). For three types of mitochondrial competitive internalization, mitochondria were stained with MitoTracker™ Deep Red FM, MitoTracker™ Green FM, and MitoTracker™ Red CMXRos for 30 minutes, washed twice with DPBS, and co-cultured with recipient cells for 24 hours. The medium was then replaced, and live-cell imaging was performed under the same conditions.

■ HIIT functional training

Six-month-old mice underwent one week of preconditioning exercise using a small animal treadmill (XR-PT-10B, Shxinruan) before beginning an 8-weeks HIIT training regimen. The maximum exercise capacity was tested weekly to adjust running speed. Each session began with a 10-minute warm-up at a speed of 10 m/min. For the first two weeks, the regimen included high-intensity exercise at 24 m/min (80% VO_2max) for 3 minutes, followed by 3 minutes of low-intensity recovery at 15 m/min with a 0° incline. In weeks 3-4, the regimen increased to 26 m/min (80% VO_2max) for 3 minutes and 15 m/min for 3 minutes at an 8° incline. In weeks 5-6, the speed was further increased to 28 m/min (80% VO_2max) for 3 minutes, followed by 17 m/min for 3 minutes at a 16° incline. Finally, in weeks 7-8, the speed reached 30 m/min (80% VO_2max) for 3 minutes, followed by 17 m/min for 3 minutes at a 25° incline. Each session concluded with 8 minutes at 15 m/min. The regimen consisted of 7 sets (3+3) per session, with each session lasting 1 hour, 5 days per week, with 2 days of rest. Similarly, a 29-years-old healthy human (the author) underwent an 8-week HIIT training program, consisting of a 30-second maximal effort sprint (9+ on the 1– 10 RPE scale) followed by a 4.5-minute low-intensity jog (4–5 on the 1–10 RPE scale), daily for 30 minutes, 5 days per week, with an additional 2 days of MICT running at 15 km/h for 30 minutes.

■ Aging model

Two categories were used: disease-induced and normal aging. For the disease-induced model, 54 two-months-old C57BL/6J mice were divided into

groups: D-gal, C2C12, Young C57, Trained People, Trained C57, and Wild Mice. Aging was induced by subcutaneous injection of D-gal at a dose of 500 mg/kg, once daily for 8 weeks. For the normal aging model, 27 four-months-old C57BL/6J mice were divided into Control, Young C57, and Wild Mice groups, with no drug treatment, and were kept under standard conditions.

■ Acute inflammation model

Two categories were used. For the inflammation model, 27 four-months-old C57BL/6J mice were divided into LPS, Young C57, and Wild Mice groups. Acute inflammation was induced by intraperitoneal injection of LPS at a dose of 2.5 mg/kg/day for 5 consecutive days. Another set of 27 four-months-old C57BL/6J mice was divided into Control, Young C57, and wild mice groups, with no drug treatment and normal rearing.

■ Animal mitochondrial transplantation

For the aging model, mitochondria were isolated from the gastrocnemius muscle tissues of Young C57, Trained People, Trained C57, and Wild Mice, as well as C2C12 cells, using the Mitochondria-Cytosol Protein Isolation Kit (C0010-50, Applygen). Mitochondrial protein was quantified using the BCA Protein Assay Kit (23250, ThermoFisher). A dose of 100 μL/100 μg of mitochondria was injected via the tail vein into the C2C12, Young C57, Trained People, Trained C57, and Wild Mice groups, while the control group received no treatment. For the normal type, mitochondria from Young C57 and Wild Mice were injected into their respective groups at the same dose, with the control group receiving 100 μL of mitochondrial carrier solution. For the acute inflammation model, mitochondria were isolated from the gastrocnemius muscle of Young C57 and Wild Mice, quantified, and injected via the tail vein at a dose of 100 μL/100 μg into the Young C57 and Wild Mice groups. The LPS group received no treatment, and the control group received 100 μL of mitochondrial carrier solution.

■ Mitochondrial biodistribution

Isolated mitochondria were labeled with MitoTracker™ Deep Red FM at room temperature for 20 minutes, washed twice with DPBS, and injected via the tail vein into mice. After 24 hours, the heart, liver, and kidneys were collected, and mitochondrial biodistribution was assessed using a multimodal small animal in vivo imaging system, PerkinElmer IVIS Spectrum (PerkinElmer).

■ Motor function detection (Rotarod Test)

Three days prior to the experiment, mice underwent adaptive training. During the formal experiment, mice were placed on a Rotating rod instrument (XR-6C/XR-6D, Shxinruan) at 5 rpm/min for 5 minutes, then gradually accelerated to 40 rpm/min. The time the mice remained on the rotating rod was recorded using a stopwatch until they fell off. The maximum duration for aging or acute inflammation mice was 180 seconds, with a maximum of 360 seconds for normal mice. Each mouse was tested three times with a 3-minutes interval between trials, ensuring a quiet environment during the experiment.

■ Body weight measurement

All experimental groups of mice were weighed 3 days before and 1 week after mitochondrial transplantation, with weights recorded.

■ Mouse forelimb grip strength test

Three days prior to the experiment, mice underwent adaptive training. During the formal experiment, each mouse was placed on a Mouse grip tester (XR501, Shxinruan), and gentle traction was applied to the tail, prompting the mouse to grip the probe firmly with its forelimbs. The grip strength reading was recorded when the experimenter applied maximum force, with the experiment conducted in a quiet environment.

■ Lower limb muscle volume and injury assessment

One week after mitochondrial injection, mice were briefly anesthetized with a mixture of isoflurane (3.0%) and O_2 (2.0 L/min) via a nose cone and placed in a custom-made restraint tube, with the right lower limb fixed with a coil. During MRI imaging, mice were anesthetized with a mixture of isoflurane (1.5%) and O_2 (0.6 L/min). The rectal temperature was maintained at 37°C ± 1°C using a heated water blanket. A small animal magnetic resonance imaging system, PharmaScan70/16S (Bruker), was used to scan the horizontal plane of lower limb muscles, employing Spin Echo (SE) T1WI (TR4000 ms, TE 28.5 ms), Fast Spin Echo (FSE) T2WI (TR4000 ms, TE 47.5 ms), with a slice thickness of 4 mm and an interval of 1 mm. Process the images using Paravision 6.0.1 (Bruker).

■ Western blot

Proteins were extracted from liver and kidney tissues, separated by 10% SDS-PAGE, and transferred onto Polyvinylidene Fluoride (PVDF) membranes. Phosphorylated proteins and total proteins were blocked with 5% BSA and 5% milk, respectively. PVDF membranes were incubated with primary antibodies at 4°C overnight, followed by a 2-hours incubation with HRP-conjugated secondary

antibodies at room temperature. Gel imaging was performed using the Tanon-5200 Multi Automatic Luminous System (Tanon).

■ Quantitative PCR

Twenty-four hours after mitochondrial transplantation, total RNA was extracted using Trizol reagent. Purified RNA was reverse-transcribed into cDNA using the PrimeScript™ RT reagent Kit (RR037Q, Takara). RT-qPCR was conducted with SYBR Green Master Mix (430915, Invitrogen) using the ABI QuantStudio 5 Real-Time PCR system (ThermoFisher). Expression levels were normalized to the internal control 18s rRNA. The primer sets are listed in key resources table.

Conclusion

■ Quantification and statistical analysis

Cell experiments were repeated at least three times except for mitochondrial competitive internalization and animal experiments except for body weight measurement, grip strength and motor function tests. GraphPad Prism 9.01(GraphPad Software Inc., San Diego, CA, USA) software was used for statistical analysis. The data were expressed as Mean ± Standard Error (SEM). For normally distributed data and comparisons between two groups, the significance was calculated using unpaired two-tailed Student's t-tests. Comparisons between three or more groups were performed using ordinary One-way ANOVA, using two-way ANOVA and Bonferroni post hoc test were used to compare multi-factor variance for multiple data. The significance threshold was determined by p value < 0.05, and the annotation was

ns = no statistical significance, * = $p<0.05$, ** = $p<0.01$, *** = $p<0.001$,**** = $p<0.0001$.

Acknowledgments

I sincerely thank the People's Hospital of Dongguan City, affiliated with Southern Medical University, for providing free access to experimental instruments. I also extend our gratitude to Dr. Guiming Chen from the Department of Pathology and Pathophysiology at Southern Medical University and Dr. Rong Wu from the School of Traditional Chinese Medicine for their technical support with mitochondrial tail vein injections. Additionally, I appreciate the assistance of Master Xin Heng in the experiments involving fluorescence microscopy for detecting reactive oxygen species and mitochondrial membrane potential. Moreover, I express strong condemnation towards those who deliberately sabotage others' experiments. I urge all laboratories to actively remove such unethical individuals. This work was carried out with the author's full commitment, with all funding provided personally by the author. Consequently, there are several limitations in this study, for which we apologize. There are three main reasons why further experiments are challenging for me: first, the experimental cells were deliberately destroyed, preventing continuation; second, it is extremely difficult to obtain mitochondria from HIIT-trained and wild mice; third, and most importantly, there is a lack of funding. Due to my poor English proficiency, this paper was translated from Chinese to English by ChatGPT for submission. If there is anything unclear, please feel free to contact me. Alternatively, you can request the original Chinese manuscript and translate it yourselves. I can also add an additional corresponding author if needed. Let me know if you need any further adjustments! Should additional resources become available, I plan to conduct more detailed research to provide a more comprehensive explanation of my study.

Author contribution

Xiaomeng Lu(fylxmgg@gmail.com) leads all the experimental design, experimental operation, experimental analysis, article writing and proofreading. JiangYong(18675838414@163.com) provided the experimental site and some experimental equipment.

Declaration of Interests

The authors declare no competing interests.

References

1. McCully JD, Cowan DB, Pacak CA, et al. Injection of isolated mitochondria during early reperfusion for cardioprotection. Am J Physiol Heart Circ Physiol. 296:94-105(2009)
2. Gorick C, Debski A. Mitochondrial transplantation for ischemic heart disease. Nat Nanotechnol.11:1-2 (2024)
3. Moskowitzova K, Shin B, Liu K, et al. Mitochondrial transplantation prolongs cold ischemia time in murine heart transplantation. J. Heart Lung Transplant. 38:92-99 (2019)
4. Sun L, Zhao Z, Guo J, et al. Mitochondrial transplantation confers protection against the effects of ischemic stroke by repressing microglial pyroptosis and promoting neurogenesis. Neural Regen Res.19:1325-1335(2024)
5. Eo H, Yu SH, Choi Y, et al. Mitochondrial transplantation exhibits neuroprotective effects and improves behavioral deficits in an animal model of Parkinson's disease. Neurotherapeutics 21:e00355 (2024)
6. Zhu Z, Li X, Wang X, et al. Photobiomodulation augments the effects of mitochondrial transplantation in the treatment of spinal cord injury in rats by facilitating mitochondrial transfer to neurons via Connexin 36. Bioeng Transl Med 8:e10473 (2023)
7. Su Y, Zhu L, Yu X, et al. Mitochondrial transplantation attenuates airway hyperresponsiveness by inhibition of cholinergic hyperactivity. Theranostics 6:1244-1260 (2016)
8. Ulger O, Kubat GB, Cicek Z, et al. The effects of mitochondrial transplantation in acetaminophen-induced liver toxicity in rats. Life Sci. 279:119669 (2021)
9. Lee JM, Hwang JW, Kim MJ, et al. Mitochondrial transplantation modulates inflammation and apoptosis, alleviating tendinopathy both in vivo and in vitro. Antioxidants.10:696 (2021)
10. Li Z, Cao X, Liu Z, et al. Therapeutic effect of mitochondrial transplantation on burn injury. Free Radic Biol Med 215:2-13(2024)
11. Kim S, Noh JH, Lee MJ, et al. Effects of Mitochondrial Transplantation on Transcriptomics in a Polymicrobial Sepsis Model. Int J Mol Sci.24:15326 (2023)
12. Cruz-Gregorio A, Aranda-Rivera AK, Amador-Martinez I, et al. Mitochondrial transplantation strategies in multifaceted induction of cancer cell death. Life Sci. 19:122098 (2023)
13. Hosseinian S, Pour PA, Kheradvar A. Prospects of mitochondrial transplantation in clinical medicine: Aspirations and challenges. Mitochondrion 65:33-44 (2022)
14. Boutonnet L, Mallard J, Charles AL, et al. Autologous mitochondrial transplantation in male mice as a strategy to prevent deleterious effects of peripheral ischemia-reperfusion. Am J Physiol Cell Physiol. 326:449-456 (2024)
15. Gray MW, Burger G, Lang BF. Mitochondrial evolution. Science 283:1476-1481(1999)
16. Schatz G. The fires of life. Annu Rev Biochem 81:34-59(2012)
17. Jiang XP, Elliott RL, Head JF. Exogenous normal mammary epithelial mitochondria suppress glycolytic metabolism and glucose uptake of human breast cancer cells. Breast Cancer Res Treat 153:519-529 (2015)
18. Ali Pour P, Kenney MC, Kheradvar A. Bioenergetics consequences of mitochondrial transplantation in cardiomyocytes. J Am Heart Assoc.9:e014501(2020)
19. Doulamis IP, Guariento A, Duignan T, et al. Mitochondrial transplantation for myocardial protection in diabetic hearts. Eur J Cardio Thorac Surg. 57:836-845.(2020)
20. Sun C, Liu X, Wang B, et al. Endocytosis-mediated mitochondrial transplantation: Transferring normal human astrocytic mitochondria into glioma cells rescues aerobic respiration and enhances radiosensitivity. Theranostics. 9:3595-3607 (2019)
21. Chang JC, Chang HS, Wu YC, et al. Mitochondrial transplantation regulates antitumour activity, chemoresistance and mitochondrial dynamics in breast cancer. J Exp Clin Cancer Res.38:1-6 (2019)
22. Sun X, Gao R, Li W, et al. Alda-1 treatment promotes the therapeutic effect of mitochondrial transplantation for myocardial ischemia-reperfusion injury. Bioact. mater.6:2058-2069 (2021)
23. Chen T, Majerníková NA, Marmolejo-Garza A, et al. Mitochondrial transplantation rescues neuronal cells from ferroptosis. Free Radical Biology and Medicine. 208:62-72 (2023)
24. Yao X, Ma Y, Zhou W, et al. In-cytoplasm mitochondrial transplantation for mesenchymal stem cells engineering and tissue regeneration. Bioeng Transl Med 7:e10250 (2022)
25. Yu Z, Hou Y, Zhou W, et al. The effect of mitochondrial transplantation therapy from different gender on inhibiting cell proliferation of malignant melanoma. Int J Biol Sci 17(2021)
26. Bhattacharya D, Slavin MB, Hood DA. Muscle mitochondrial transplantation can rescue and maintain cellular homeostasis. Am J Physiol Cell Physiol. 325:862-884 (2023)
27. Picone P, Porcelli G, Bavisotto CC, et al. Synaptosomes: new vesicles for neuronal mitochondrial transplantation. J Nanobiotechnology. 19:1-5(2021)
28. Baharvand F, Roudkenar MH, Pourmohammadi-Bejarpasi Z, et al. Safety and efficacy of platelet-derived mitochondrial transplantation in ischaemic heart disease. Int j cardiol. 410:132227 (2024)
29. Bamshad C, Roudkenar MH, Abedinzade M, et al. Human umbilical cord-derived mesenchymal stem cells-harvested mitochondrial transplantation improved motor function in TBI models through rescuing neuronal cells from apoptosis and alleviating astrogliosis and microglia activation. Int Immunopharmacol. 118:110106 (2023)
30. Guariento A, Piekarski BL, Doulamis IP, et al. Autologous mitochondrial transplantation for cardiogenic shock in pediatric patients following ischemia-reperfusion injury. J Thorac Cardiovasc Surg. 162(3):992-1001 (2021)
31. Dubinin MV, Mikheeva IB, Stepanova AE, et al. Mitochondrial Transplantation Therapy Ameliorates Muscular Dystrophy in mdx Mouse Model. Biomolecules 14:36 (2024)
32. Kaza AK, Wamala I, Friehs I, et al. Myocardial rescue with autologous mitochondrial transplantation in a porcine model of ischemia/reperfusion. J Thorac Cardiovasc Surg. 153:934-943 (2017)
33. Javani G, Babri S, Farajdokht F, et al. Mitochondrial transplantation improves anxiety-and depression-like behaviors in aged stress-exposed rats. Mech Ageing Dev. 202:111632 (2022)
34. Broughton RE, Reneau PC. Spatial covariation of mutation and nonsynonymous substitution rates in vertebrate mitochondrial genomes. Mol Biol Evol 23:1516-1524(2006)
35. Mahler HR. Mitochondrial evolution: organization and regulation of mitochondrial genes. Ann N Y Acad. Sci 361:53-75.(1981)
36. Logan DC. The mitochondrial compartment. J Exp Bot 57:1225-1243(2006)
37. Gray MW. Mitochondrial evolution. Cold Spring Harbor perspectives in biology. 4:a011403 (2012)
38. Burki F. Mitochondrial evolution: going, going, gone. Curr Biol. 26:410-412 (2016)
39. Raval PK, Martin WF, Gould SB. Mitochondrial evolution: Gene shuffling, endosymbiosis, and signaling. Sci Adv 9:eadj4493. (2023)
40. Butenko A, Lukeš J, Speijer D, et al. Mitochondrial genomes revisited: why do different lineages retain different genes?. BMC Biol 22:15 (2024)
41. Levoux J, Prola A, Lafuste P, et al. Platelets facilitate the wound-healing capability of mesenchymal stem cells by mitochondrial transfer and metabolic reprogramming. Cell Metab 33:283-299 (2021)
42. Zhang A, Liu Y, Pan J, et al. Delivery of mitochondria confers cardioprotection through mitochondria replenishment and metabolic compliance. Mol. Ther 31:1468-1479 (2023)
43. Jin M, Wang Y, Huang M, et al. Sulphation can enhance the antioxidant activity of polysaccharides produced by Enterobacter cloacae Z0206. Carbohydr Polym.. 99:624-629 (2014)
44. Ganote CE, Armstrong SC. Effects of CCCP-induced mitochondrial uncoupling and cyclosporin A on cell volume, cell injury and preconditioning protection of isolated rabbit cardiomyocytes. J Mol Cell Cardiol.35:749-759 (2003)
45. Fuchs CD, Radun R, Dixon ED et al. Hepatocyte-specific deletion of adipose triglyceride lipase (adipose triglyceride lipase/patatin-like phospholipase domain containing

2) ameliorates dietary induced steatohepatitis in mice. Hepatology Jan;75:125-139 (2022

46. Clark MA, Shay JW. Mitochondrial transformation of mammalian cells. Nature 295:605-607 (1982)
47. Song JH, Choi J, Hong YJ et al. Developmental Potency and Metabolic Traits of Extended Pluripotency Are Faithfully Transferred to Somatic Cells via Cell Fusion-Induced Reprogramming. Cells. 11:3266 (2022)
48. Reznick DN, Ricklefs RE. Darwin's bridge between microevolution and macroevolution. Nature. 457:837-842 (2009)
49. Hsu CC, Wang CH, Wu LC, et al. Mitochondrial dysfunction represses HIF-1α protein synthesis through AMPK activation in human hepatoma HepG2 cells. Biochim Biophys Acta (BBA)-Gen Subj.1830:4743-4751 (2013)
50. Volchuk A, Ye A, Chi L, et al. Indirect regulation of HMGB1 release by gasdermin D. Nat Commun 11:4561(2020)
51. Hu YM, Lu SZ, Li YS et al. Protective effect of antioxidant peptides from grass carp scale gelatin on the H2O2-mediated oxidative injured HepG2 cells. Food Chem. 373:131539(2022)
52. Doulamis IP, Nomoto RS, Tzani A, et al. Transcriptomic and proteomic pathways of diabetic and non-diabetic mitochondrial transplantation. Sci Rep. 12:22101 (2022)
53. McCully JD, Del Nido PJ, Emani SM. Mitochondrial transplantation: the advance to therapeutic application and molecular modulation. Front Cardiovasc Med.10:1268814 (2023)
54. Tripathi K, Ben-Shachar D. Mitochondria in the Central Nervous System in Health and Disease: The Puzzle of the Therapeutic Potential of Mitochondrial Transplantation. Cells. 13:410 (2024)
55. Hong S, Kim S, Kim K, Lee H. Clinical approaches for mitochondrial diseases. Cells. 12:2494 (2023)
56. La Morgia C, Maresca A, Caporali L, et al. Mitochondrial diseases in adults. J Intern Med 287:592-608 (2020)
57. Nitsch L, Lareau CA, Ludwig LS. Mitochondrial genetics through the lens of single-cell multi-omics. Nature genetics. 56:1355-1365 (2024)
58. Shang Q, Bian X, Zhu L et al. Lactate Mediates High-Intensity Interval Training—Induced Promotion of Hippocampal Mitochondrial Function through the GPR81-ERK1/2 Pathway. Antioxidants. 12:2087 (2023)
59. Souza-Tavares, H., Santana-Oliveira, et al. Exercise enhances hepatic mitochondrial structure and function while preventing endoplasmic reticulum stress and metabolic dysfunction-associated steatotic liver disease in mice fed a high-fat diet. Nutr Res, 126, pp.180-192 (2024)
60. Jiang X, Ji S, Yuan F, et al. Pyruvate dehydrogenase B regulates myogenic differentiation via the FoxP1–Arih2 axis. J Cachexia Sarcopenia Muscle. 14:606-621 (2023)
61. Fu Y, Liu H, Song C, et al. Mangiferin regulates cognitive deficits and heme oxygenase-1 induced by lipopolysaccharide in mice. Int. Immunopharmacol. 29:950-956(2015)
62. Lelandais C, Albert B, Gutierres S et al. Organization and expression of the mitochondrial genome in the Nicotiana sylvestris CMSII mutant. Genetics. 150:873-882 (1998)
63. Cohen NR, Lobritz MA, Collins JJ. Microbial persistence and the road to drug resistance. Cell Host Microbe 13:632-642 (2013)
64. Jin P, Jiang J, Zhou L et al. Mitochondrial adaptation in cancer drug resistance: prevalence, mechanisms, and management. J Hematol Oncol. 15:97 (2022)